[4] T. Head-Gordon, *Proc. Natl Acad. Sci. USA* **1995**, *92*, 8308; D. T. Bowron, A. Filipponi, M. A. Roberts, J. L. Finney, *Phys. Rev. Lett.* **1998**, *81*, 4164.
[5] G. A. Jeffrey in *Inclusion Compounds*, *Vol. 1* (Eds.: J. L. Atwood, J. E. D. Davies, D. D. MacNicol), Academic Press, London, **1984**, 135.
[6] J. A. Ripmeester, C. I. Ratcliffe, J. S. Tse, B. M. Powell, *Nature* **1987**, *325*, 135; K. A. Udachin, C. I. Ratcliffe, G. D. Enright, J. A. Ripmeester, *Supramol. Chem.* **1997**, *8*, 173.
[7] K. A. Udachin, J. A. Ripmeester, *Nature* **1999**, *397*, 420.
[8] D. W. Davidson in *Water, A Comprehensive Series* (Ed.: F. Franks), Plenum, New York, **1972**.
[9] Y. A. Dyadin, F. V. Zhurko, I. V. Bondaryuk, G. O. Zhurko, *J. Inclusion Phenom.* **1991**, *10*, 39.
[10] S. L. Miller, S. R. Gough, D. W. Davidson, *J. Phys. Chem.* **1977**, *81*, 2154.
[11] S. R. Gough, S. K. Garg, J. A. Ripmeester, D. W. Davidson, *J. Phys. Chem.* **1977**, *81*, 2158.
[12] K. A. Udachin, G. D. Enright, C. I. Ratcliffe, J. A. Ripmeester, *J. Am. Chem. Soc.* **1997**, *119*, 11481.
[13] Dimethyl ether hydrate is trigonal, space group $P321$, $a = 34.995$, $c = 12.368$ Å, $\gamma = 120°$, $V = 13117.7$ Å^3, $Z = 48$, GOF on $F^2 = 0.962$. Final R indeces ($I > 2\sigma(I)$): $R_1 = 0.0538$, $wR_2 = 0.1062$ (145366 total reflections, 22397 unique).
[14] H. Gies in *Inclusion Compounds*, *Vol. 5* (Eds.: J. L. Atwood, J. E. D. Davies, D. D. MacNicol), Oxford University Press, **1991**, p. 1.
[15] M. J. Collins, C. I. Ratcliffe, J. A. Ripmeester, *J. Phys. Chem.* **1990**, *94*, 157; J. A. Ripmeester, C. I. Ratcliffe, *Comprehensive Supramolecular Chemistry*, *Vol. 8* (Eds.: J. E. D. Davies, J. A. Ripmeester), Pergamon/Elsevier, Oxford, **1996**.
[16] J. A. Ripmeester, C. I. Ratcliffe, *J. Phys. Chem.* **1990**, *94*, 8773.
[17] G. M. Sheldrick, *Acta Crystallogr. Sect. A* **1990**, *46*, 467.
[18] Additional crystallographic information: Solved by direct method using the SHELXTL suite of programs.[17] TWIN matrix 010 100 00-1 was used to resolve the crystal twinning. All non-hydrogen atoms were refined anisotropically by full-matrix least squares on F^2. Hydrogen atoms in the water framework were found from the electron density map and are disordered over two positions in a hydrogen bond with a site occupancy of 0.5. Hydrogen atoms in the guest molecules were placed in calculated positions and allowed to ride on the parent atoms. All C–O and C–C bonds in guest molecules were fixed. No corrections were made for polarization or absorption.

The Oxidative Power of Protonated Hydrogen Peroxide**

Åse M. Leere Øiestad, Allan C. Petersen, Vebjørn Bakken, John Vedde, and Einar Uggerud*

Hydrogen peroxide is an oxidant which receives much attention these days. In order to take full advantage of this environmentally friendly chemical in a large number of practical applications—for example, for bleaching in the pulp and paper industry—more effective catalysts are required.[1] Detailed mechanistic studies of simplified model systems are necessary to realize this development.

The compound H_2O_2 is unstable and decomposes into water and dioxygen (O_2) in both acidic and basic solution, as well as in the presence of transition metals.[2] Good examples of transition metal activation occur with Fenton's reagent (Fe^{2+} and H_2O_2) as well as the enzymes involved in respiration and other oxidative processes.[3–5] The fine balance between the decomposition chemistry of H_2O_2 and its action as an oxidant is quite clear, both when it is promoted by protonation or by coordination to a transition metal cation. We have recently proposed that $[HOOH]H^+$, the species most likely to be formed in acidic hydrogen peroxide solution, is a highly active oxidant in the gas phase; only 150 kJ mol^{-1} are needed to break the O–O bond.[6]

Hydrogen peroxide demonstrates extraordinary oxidative behavior in superacidic solutions: it inserts an oxygen atom into aliphatic and aromatic C–H bonds to give aldehydes/ketones or alcohols, respectively.[7–9] Theoretical calculations indicate that the reactive species is protonated hydrogen peroxide, and not free OH^+.[10] To date, no experimental evidence has been published that demonstrates the intrinsic chemical properties of $HOOH_2^+$, but it is known that this species can be formed by proton transfer in the gas phase (a rough value of 675 ± 45 kJ mol^{-1} was reported for the proton affinity (PA) of H_2O_2).[11] Herein we present the results from an experimental study of the unimolecular and bimolecular gas-phase chemistry of protonated hydrogen peroxide.

We have previously investigated the unimolecular chemistry of the isoelectronic $[H_2NNH_2]H^+$ and $[HONH_2]H^+$ systems.[12, 13] On the basis of the behavior of these ions and from a detailed quantum chemical survey of the singlet and triplet potential energy surfaces of $(H_3,O_2)^+$ we recently proposed that protonated hydrogen peroxide in its singlet ground state will preferably lose an oxygen atom according to the spin change mechanism [Eq. (1)].[6]

$$\begin{aligned} {}^1HOOH_2^+ &\rightarrow {}^1HO\cdots OH_2^+ \rightarrow {}^3HO\cdots OH_2^+ \\ &\rightarrow {}^3O\cdots H_3O^+ \rightarrow {}^3O + H_3O^+ \end{aligned} \quad (1)$$

We have now conducted experiments on a grand-scale magnetic sector tandem mass spectrometer to verify this prediction. A pure beam of $[HOOH]H^+$ ions (m/z 35.01) was selected using the first mass spectrometer of the tandem combination. A small fraction of these ions, with energies close to the threshold value for reaction (the so-called metastable ions), decompose spontaneously during passage through the field-free region preceding the second mass spectrometer, and the fragment ions were registered by scanning the second electric sector. The spectrum obtained is shown in Figure 1. the spectrum contains only one significant peak, namely for H_3O^+, which corresponds to the loss of one oxygen atom, and is in complete agreement with the theoretical predictions. The maximum amount of energy available to the $HOOH_2^+$ ions produced in the ion source

[*] Prof. Dr. E. Uggerud, Å. M. Leere Øiestad, V. Bakken, J. Vedde
Department of Chemistry, University of Oslo
P. O. Box 1033 Blindern, 0315 Oslo (Norway)
Fax: (+47) 22-85-54-41
E-mail: einar.uggerud@kjemi.uio.no.
A. C. Petersen
Department of Chemistry, University of Copenhagen
Universitetsparken 5, 2100 Copenhagen (Denmark)

[**] The work was supported by NFR (The Norwegian Research Council). The authors thank Drs. Gustav Bojesen and Steen Hammerum (University of Copenhagen) for generous cooperation, and Prof. H. Bernhard Schlegel (Wayne State University) for computer time and the use of a development version of Gaussian 98. Helpful suggestions from Profs. Terry B. McMahon (Waterloo University) and Michael T. Bowers (UC, Santa Barbara) are acknowledged.

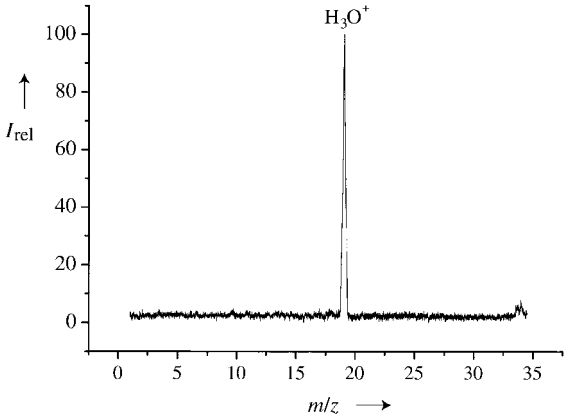

Figure 1. Metastable ion kinetic energy spectrum (see text for explanation) of protonated hydrogen peroxide (m/z 35). Reactant ions were accelerated by an electric potential difference of 6 kV. The translational energy release, which is obtained from the width of the peak at half height, is $T_{0.5} = 8\,kJ\,mol^{-1}$. The small peak at m/z 34 arises from collisional activation with residual gas in the analyzer tube (7×10^{-8} mbar). Separate experiments show that the peak at m/z 34 dominates the collisional activation spectrum. The observed peaks are m/z (relative intensity, collision gas He): 34 (100), 33 (8), 32 (9), 19 (27), 18 (25), 17 (10), 16 (2). In addition, there is a narrow signal for m/z 17.5, which corresponds to $HOOH_2^{2+}$, and is more prominent when O_2 is used as the collision gas.

under the conditions employed is around 150 kJ mol^{-1}. This value corresponds to the difference in proton affinity between methane (the ionizing agent is CH_5^+) and hydrogen peroxide (Table 1[10, 14, 15]), and includes 20 kJ mol^{-1} as an estimated upper limit to the available thermal energy.

Table 1. Reaction data.

Compound	PA[a] [kJ mol^{-1}]	$\Delta H^\ominus$ for H^- transfer[b] [kJ mol^{-1}]	E_{crit}[c] [kJ mol^{-1}]	k[d] [cm^3 molecule^{-1} s^{-1}]
CH_4	544	−31	22	$< 7 \times 10^{-13}$
C_2H_6[e]	596	−214	1	4.9×10^{-11}
C_3H_8	626	−306	−19	3.6×10^{-10}
iC_4H_{10}	678	−372	−21	1.3×10^{-9}
H_2O_2	675	–	–	–

[a] Proton affinity (data from ref. [14]). [b] Standard enthalpy change for hydride transfer [Eq. (2); data from ref. [15]]. [c] Calculated critical energy (barrier height; data from ref. [10]). [d] Rate coefficient [Eq. (2)] for this work, estimated standard deviations: 20% (absolute). [e] Deuterium-labeling experiments showed that a second reaction channel is operative giving $H_3O^+ + C_2H_4 + H_2O$, with a rate coefficient of less than 3% relative to the dominating $C_2H_5^+$-producing reaction.

The O–O bond dissociation energy of neutral HOOH is 214 kJ mol^{-1}.[15] The present experiment in conjunction with the theoretical model suggests that the effective barrier for bond dissociation of $HOOH_2^+$ is ≤ 150 kJ mol^{-1}, which shows that protonation activates the hydrogen peroxide molecule considerably. It is noticeable that the neutral product of Equation (1) is oxygen in its triplet electronic state. This atom, and the corresponding isoelectronic triplet NH and CH_2 species, are well known to insert into C–H bonds.

Bimolecular reactions between $HOOH_2^+$ and alkanes were investigated using a Fourier transform ion cyclotron resonance (FT-ICR) mass spectrometer using conditions described in detail elsewhere.[16] Briefly, $HOOH_2^+$ ions were produced in an external ion source, transferred to the cell of the instrument, isolated, thermalized, reacted with the alkane, and the reaction rates were determined by recording FT-ICR mass spectra at different reaction times.

The key reaction data are given in Table 1, and a typical mass spectrum is shown in Figure 2. With the exception of

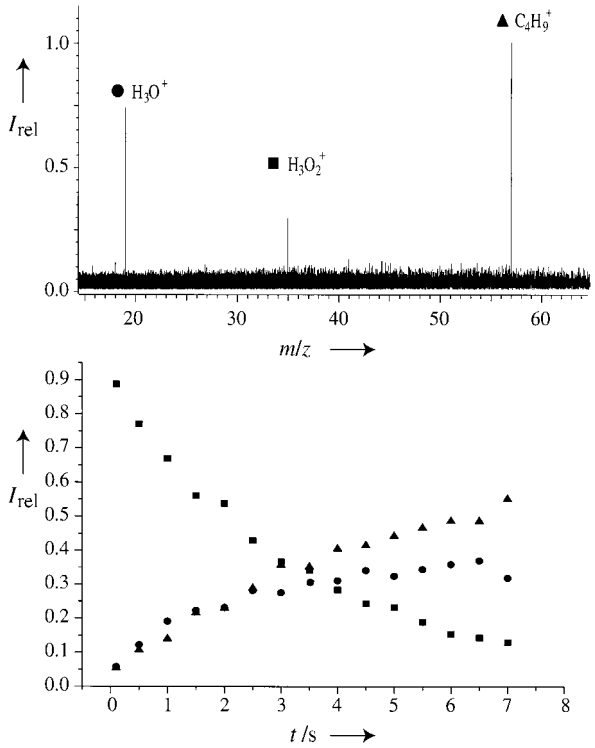

Figure 2. Top: Mass spectrum obtained after 5.5 s reaction between $HOOH_2^+$ and isobutane at 5×10^{-9} mbar. The signal for H_3O^+ at m/z 19 arises from fast proton transfer with background water. Bottom: The temporal dependence of the reactant ion signal and the two product ions.

methane, all the alkanes investigated underwent reaction according to Equation (2).

$$RH + HOOH_2^+ \rightarrow R^+ + 2\,H_2O \qquad (2)$$

There are several noticeable features of these results: Firstly, *n*-butane and isobutane are known to be oxidized to the corresponding alcohols by hydrogen peroxide in superacid,[8] while in the gas phase even ethane and propane react. Secondly, the reaction product collected in superacid is the alcohol, which means that an O atom has been inserted into the C–H bond. In the gas phase the product is the corresponding alkyl cation, which means that a hydride ion has been abstracted from the alkane. The alternative, namely proton transfer to the alkane followed by dihydrogen loss, is unlikely since Table 1 shows that proton transfer is endothermic, except for isobutane.

Bach and Su have presented a quantum chemical model to account for the observations from the experiments performed in superacid solution.[10] Interestingly, the properties of the transition state they identified imply that the first stage of the

  1433-7851/01/4007-1306 $ 17.50+.50/0

reaction [Eq. (3)] is hydride abstraction from the alkane by $HOOH_2^+$.

$$RH + HOOH_2^+ \rightarrow ROH_2^+ + H_2O \quad (3)$$

The O–O bond breaks simultaneously, and a C–O bond is formed subsequently. Bach and Su took it for granted in their model that the final reaction product is the alcohol plus water, as observed in solution. This may at first glance seem to be inconsistent with the formation of R^+ in the gas phase, but Bach and Su did not take the full gas-phase reaction dynamics into account.

To deal with this problem, we found it pertinent to perform ab initio direct dynamics calculations[17–20] on the reaction of ethane. Our approach was the following: First, we duplicated the calculations of Bach and Su. As already indicated, the reaction coordinate obtained for the transition structure (TS) corresponds to hydride transfer from ethane to the oxygen atom of the OH part of the molecule in concert with dissociation of the O–O bond (first frame of Figure 3). Secondly, we calculated a series of ab initio direct dynamics trajectories to get an insight into how the liberated energy influences the course of the reaction. In this method Newton's equations are integrated step-by-step along the classical trajectory of a reaction. A total of 25 different trajectories, starting at the TS, were computed using randomly chosen initial conditions. The HF/6-31G(d) wave function was used.[21] One typical trajectory is presented in Figure 3. The calculations reveal that the water molecule derived from the OH_2 group of the original $HOOH_2^+$ molecule is already pushed away from the rest of the product system after passage of the TS. For a short period the remaining $C_2H_5OH_2^+$ unit may be regarded as one entity (a short-lived complex between $C_2H_5^+$ and H_2O). The large amount of energy deposited in the complex leads in 80% of the trajectories to dissociation into $C_2H_5^+$ and H_2O in less than 60 fs after generation of the TS. According to the calculations, all the complexes have dissociated within 400 fs, with the exception of one which dissociates at 900 fs. This behavior of the free gas-phase reaction differs from that in the condensed phase where surrounding molecules confine the products and also act as energy sinks, thereby giving the alcohol as the ultimate product.

When we treated fully deuterated ethane (C_2D_6) with $HOOH_2^+$ we observed that greater than 97% of the product mixture is $C_2D_5^+$ (including secondary products) and less than 3% HD_2O^+. The latter product ion is the result of proton transfer from $C_2D_5^+$ to HDO during the short lifetime of the initially formed $C_2D_5^+ \cdots HDO$ complex. This result is interesting, since it is well known that long-lived $C_2H_5^+ \cdots OH_2$ ions have a strong preference for giving the thermodynamically more-stable product H_3O^+.[22–25] In other words, our deuterium-label experiment verifies the outcome of the trajectory calculations, and shows there is an essentially nonstatistical (nonergodic) behavior in the system—at most the complex exists for a couple of vibrational periods. None of the 25 trajectories shows proton transfer to water.

In conclusion, we have found that the oxidation of alkanes by protonated hydrogen peroxide does not occur by insertion of O into C–H, but by a multistep sequence in which a simple hydride transfer is the essential step. There is an ongoing

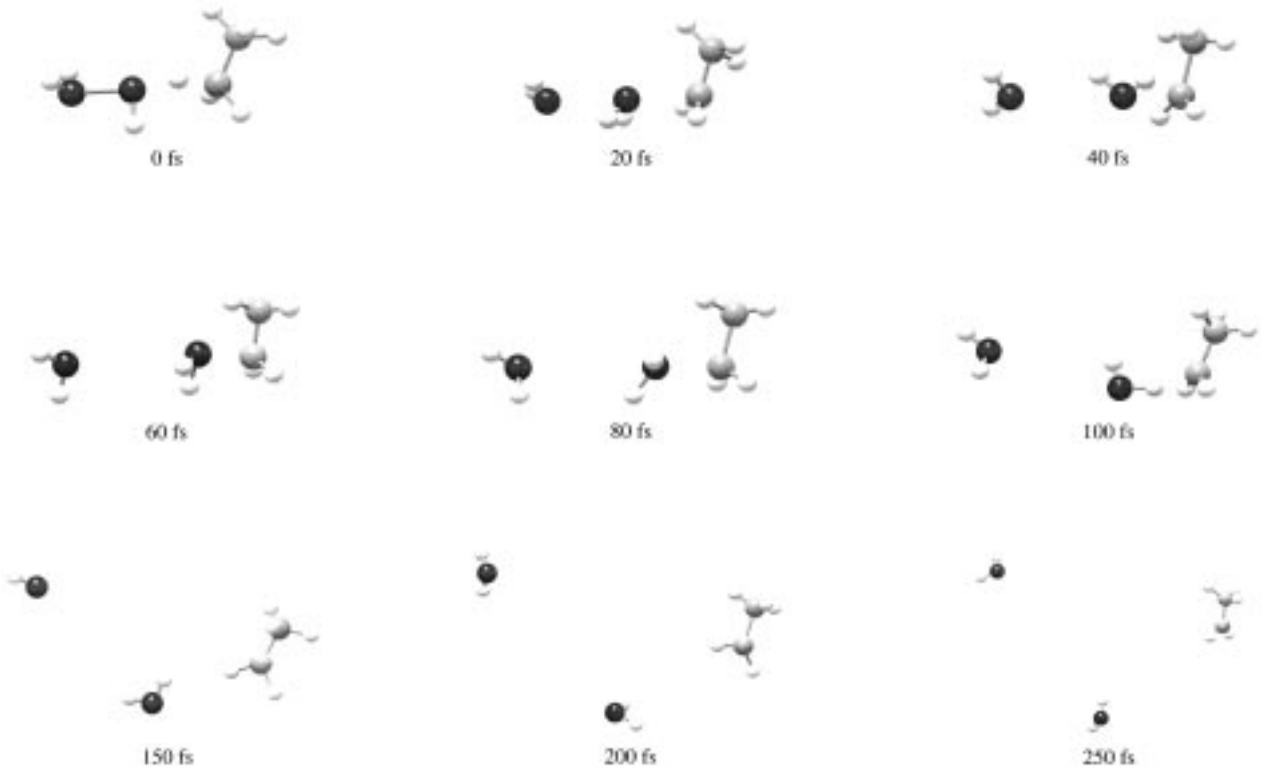

Figure 3. Images of a direct dynamics reaction trajectory (HF/6-31G(d)) for $HOOH_2^+ + C_2H_6 \rightarrow C_2H_5^+ + 2H_2O$. Images are shown from $t = 0$ (transition state) up to 250 fs. The colour codings are H: white, C: light gray, and O: dark gray.

  1433-7851/01/4007-1307 $ 17.50+.50/0

discussion about the mechanism of the activation of iron cations in Fenton chemistry and in related enzymes. We think that the present findings point towards the $Fe(OH)OH^+$ structural motif as the active species in these systems.[3–5]

The above discussion showed that the first stage of Equation (2) corresponds to a concerted hydride abstraction/water loss mechanism. It may be regarded as an S_N2 reaction type and it provides a hint for regarding protonated hydrogen peroxide as a charge-transfer complex formed between OH^+ and H_2O. The analogy to protonated laughing gas (N_2OH^+)[26] and protonated ozone (O_3H^+)[27] on one hand, and protonated methanol ($CH_3OH_2^+$)[28] on the other is evident. From this point of view it became pertinent to see how easily $HOOH_2^+$ reacts in more typical S_N2 reactions. The natural prototype would be the identity substitution reaction [Eq. (4)].

$$\mathbf{H_2O} + HOOH_2^+ \rightarrow HO\mathbf{OH_2}^+ + H_2O \qquad (4)$$

In order to check this possibility we performed MP2/6-31G(d,p) ab initio quantum-chemical calculations.[21] The calculations (Figure 4) revealed that the reaction should have

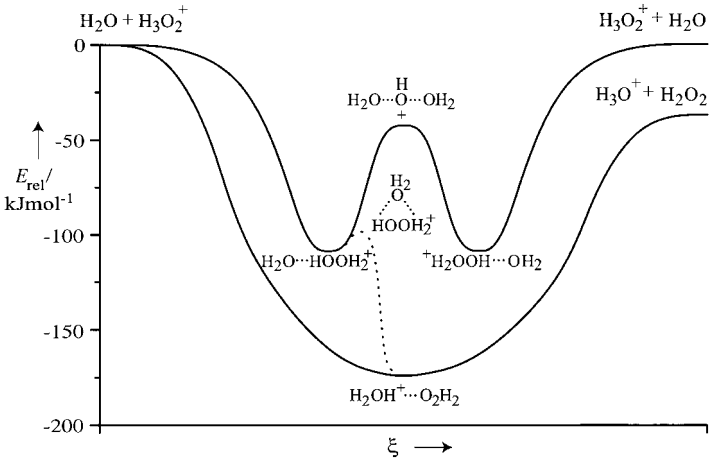

Figure 4. Potential energy diagram for the hypothetic reaction between H_2O and $HOOH_2^+$ obtained from MP2/6-31G(d,p) calculations. Relative energies are in kJ mol^{-1} and include scaled zero-point vibrational energy corrections.

a potential-energy barrier far below that of the reactants. We also considered an alternative reaction route, the proton-transfer reaction [Eq. (5)].

$$H_2O + [HOOH]\mathbf{H}^+ \rightarrow HOOH + [H_2O]\mathbf{H}^+ \qquad (5)$$

These theoretical predictions encouraged us to perform an experimental investigation of the outcome of reactions between ^{18}O-labeled water and $HOOH_2^+$ by using FT-ICR mass spectrometry. Despite the potentially promising S_N2 mechanism, it was not possible to observe any product ion incorporating ^{18}O. Instead proton transfer [Eq. (5)] is dominating as a consequence of its highly favorable entropy factor relative to the tight transition state required for a S_N2 mechanism. Proton transfer occurs efficiently, close to the theoretical collision rate limit. Our results do not rule out the occurrence of Equation (4). If it occurs, the product ion is consumed at an even faster rate through Equation (5). It is possible that $HO\mathbf{OH_2}^+$ will remain unobserved under the conditions of the experiment, even when the rate of Equation (4) is as high as 15 % of that of Equation (5). In any case, it is highly interesting and relevant that our theoretical model indicates that S_N2 reactions are feasible for molecules of this type.

Experimental Section

Protonated hydrogen peroxide was produced in a custom-made chemical ionization ion source in a four-sector (*EBEB* geometry) mass spectrometer (JMS-HX/HX110 A, JEOL Ltd.). Methane was used as the reagent gas. The source of hydrogen peroxide was a 35 wt % H_2O_2/urea formulation (Acros Chemicals) which permits the use of a direct inlet probe. The ions were accelerated (accelerating voltage 6 kV) and a pure beam of ions with m/z 35.01 at a mass resolution of 2000 was isolated with the first two sectors. A small fraction of the $HOOH_2^+$ ions selected in this manner—having an energy sufficiently close to the threshold—decompose spontaneously in the field-free region proceeding the second *E*-sector. To reach this stage these metastable ions have survived approximately 25 μs after they were formed in the ion source. The product ions formed by this spontaneous unimolecular decomposition were analyzed with the second *E*-sector, and registered by a detector mounted in the field region following that sector.

$HOOH_2^+$ ions were produced in an external ion source using chemical ionization with methane. The ions formed in the source were transferred to the cell of a Bruker 4.7 T FT-ICR instrument. All ions—except those having m/z 35—were then ejected from the cell. The remaining population of $HOOH_2^+$ ions (m/z 35.0133) were cooled to ambient temperature upon introducing a short pulse of Ar. The $HOOH_2^+$ ions were then isolated by single frequency shots that removed ions fromed during the cooling period of 4 s. After this process the ions were treated with the respective alkane ($p = 2 \times 10^{-9} - 1.5 \times 10^{-7}$ mbar) for a variable time before a mass spectrum was recorded. In this way the reaction could be followed as a function of time, and rate coefficients obtained by fitting kinetic models to the reactant deacy and formation of the product ions.

The direct ab initio approach to trajectory calculations utilizes the first and second derivatives (with respect to atomic displacements) of a general wave function within the framework of the Born–Oppenheimer approximation. Each trajectory $\boldsymbol{q}(t) = [\boldsymbol{q}(t_1), \boldsymbol{q}(t_2),\ldots]$ is calculated by a stepwise procedure which requires recalculation of the wavefunction at points $\boldsymbol{q}_i$ in time steps typically varying between 0.2 and 0.5 fs. This approach is of course very demanding in computer time; one single trajectory requires the calculation of the wave function for a large number of points. For this reason there are limits to the dimension of the wave function which can be used. In this case we were able to calculate 25 different trajectories using HF/6-31G(d), which we think is a reasonable compromise between computer time and chemical accuracy, and is a representative ensemble of the initial conditions taken from a thermal distribution at 298 K.

All quantum chemical calculations were performed using Gaussian 98.[21] A more comprehensive documentation of the results of the trajectory calculations, including movies, are exclusively available at: http://www.uio.no/~vebjornb/supmat.html.

Received: November 24, 2000 [Z16172]

[1] P. T. Anastas, T. C. Williamson, *Green Chemistry—Frontiers in Benign Chemical Syntheses and Processes*, Oxford University Press, Oxford, **1998**.
[2] F. A. Cotton, G. Wilkinson, *Advanced Inorganic Chemistry*, Wiley, New York, **1988**.
[3] J. Everse, K. E. Everse, M. B. Grisham, *Peroxidases in Biology and Chemistry*, CRC Press, Boca Raton, **1991**.

  1433-7851/01/4007-1308 $ 17.50+.50/0

[4] G. R. Ortiz de Montellano, *Cytochrome P-450. Structure, Mechanism and Biochemistry*, Plenum, New York, **1986**.
[5] S. Shaik, M. Filatov, D. Schröder, H. Schwarz, *Chem. Eur. J.* **1998**, *4*, 193 – 199.
[6] E. L. Øiestad, J. N. Harvey, E. Uggerud, *J. Phys. Chem. A* **2000**, *104*, 8382 – 8388.
[7] G. A. Olah, D. G. Parker, N. Yoneda, *J. Am. Chem. Soc.* **1977**, *99*, 483 – 488.
[8] G. A. Olah, D. G. Parker, N. Yoneda, *Angew. Chem.* **1978**, *90*, 962 – 984; *Angew. Chem. Int. Ed. Engl.* **1978**, *17*, 909 – 931.
[9] G. A. Olah, T. Keumi, J. C. Lecoq, A. P. Fung, J. A. Olah, *J. Org. Chem.* **1991**, *56*, 6148 – 6151.
[10] R. D. Bach, M.-D. Su, *J. Am. Chem. Soc.* **1994**, *116*, 10103 – 10109.
[11] W. Lindinger, D. L. Albritton, C. J. Howard, F. C. Fehsenfeld, E. E. Ferguson, *J. Chem. Phys.* **1975**, *63*, 5220 – 5222.
[12] E. L. Øiestad, E. Uggerud, *Int. J. Mass Spectrom. Ion Processes* **1997**, *165/166*, 39 – 47.
[13] E. L. Øiestad, E. Uggerud, *Int. J. Mass Spectrom.* **1999**, *185/186/187*, 231 – 240.
[14] E. P. L. Hunter, S. G. Lias, *J. Phys. Chem. Ref. Data* **1998**, *27*, 413 – 656.
[15] S. G. Lias, J. E. Bartmess, J. F. Liebman, J. H. Holmes, R. D. Levin, W. G. Mallard, *J. Phys. Chem. Ref. Data Suppl.* **1988**, *17*.
[16] L. Bache-Andreassen, E. Uggerud, *Int. J. Mass Spectrom.* **2000**, *195/196*, 171 – 184.
[17] T. Helgaker, E. Uggerud, H. J. A. Jensen, *Chem. Phys Lett.* **1990**, *173*, 145 – 150.
[18] W. Chen, W. L. Hase, H. B. Schlegel, *Chem. Phys. Lett.* **1994**, *228*, 436 – 442.
[19] J. M. Millam, V. Bakken, W. Chen, W. L. Hase, H. B. Schlegel, *J. Chem. Phys.* **1999**, *111*, 3800 – 3805.
[20] V. Bakken, J. M. Millam, H. B. Schlegel, *J. Chem. Phys.* **1999**, *111*, 8773 – 8777.
[21] Gaussian 98, Revision A.5, Gaussian Inc., Pittsburgh, PA, USA, **1998**.
[22] M. F. Jarrold, A. J. Illies, N. J. Kirchna, M. T. Bowers, *Org. Mass Spectrom.* **1983**, *18*, 388 – 395.
[23] A. Harrison, *Org. Mass Spectrom.* **1987**, *22*, 637 – 641.
[24] G. Bouchoux, Y. Hoppilliard, *J. Am. Chem. Soc.* **1990**, *112*, 9110 – 9115.
[25] D. J. Swanton, D. C. J. Marsden, L. Radom, *Org. Mass Spectrom.* **1991**, *26*, 227 – 234.
[26] J. Mestres, M. Duran, J. Bertán, E. Ballesteros, M. Herreros, J.-L. M. Abboud, *Chem. Phys.* **1995**, *192*, 99 – 110.
[27] F. Cacace, M. Speranza, *Science* **1994**, *265*, 208 – 209.
[28] L. Bache-Andreassen, E. Uggerud, *Chem. Eur. J.* **1999**, *5*, 1917 – 1930.

  1433-7851/01/4007-1309 $ 17.50+.50/0